A98-31482

ICAS-98-1,10,3

PNEUMATIC YAW CONTROL AT HIGH ANGLE OF ATTACK FOR LOW OBSERVABILITY COMBAT AIRCRAFT

K.P.Garry S.P.Williams
College of Aeronautics, Cranfield University, Bedford. MK43 OAL (UK)

Summary

A series of low speed wind tunnel tests have been conducted using a generic combat aircraft model to investigate pneumatic methods of yaw control at high angle of attack. The results show that blowing air through slots near the forebody apex can produce significant yawing moment and side force.

Light sheet flow visualisation shows that blowing modifies the forebody shear layer trajectory in such a way as to induce forebody vortex asymmetry at up to 45 degrees angle of attack. Coupling with the wing vortex system induces large rolling moments within certain incidence ranges.

Yawing moment increases with blowing momentum coefficient up to a critical value above which the blowing side forebody vortex bursts and further yawing moment increments are developed through blowing thrust effects alone. Variations in both forebody geometry and blowing direction were found to have a significant effect on the levels of yawing moment achieved.

Introduction

The development of a robust method of yaw control at high angle of attack will be required for future combat aircraft configurations. Pneumatic methods of forebody vortex manipulation offer the potential for effective yaw control while being consistent with the requirements for low observability.

This paper describes a series of wind tunnel tests on a model scale generic combat aircraft at angles of attack up to 60 degrees. The model incorporates a chined cross section forebody and flat plate, diamond planform, wing. Provision is included for slot blowing along the forebody chine edge.

The primary objectives of the programme were to; (a) identify both the angle of attack and the blowing momentum coefficient envelope of effectiveness, (b) investigate the extent of coupling between the desired yaw control and the remaining degrees of freedom, and (c) to gain an understanding of the flowfield mechanisms involved.

Experimental Arrangement

All tests were conducted in a 2.4m x 1.2m closed working section, open return wind tunnel at a free stream velocity of 20 m/s, corresponding to a nominal Reynolds number of 470,000 based on wing mean aerodynamic chord (mac).

The Cranfield High - Alpha Research Model (CHARM) consists of a highly blended chined forebody / fuselage and a flat plate, clipped diamond planform wing with all edges bevelled at 30 degrees. The leading and trailing edge sweep angles are 20 degrees and 50 degrees respectively.

Model forces and moments were obtained from an internal five component strain gauge balance. The model and balance can be assembled such that data can be obtained for the complete forebody / wing combination, the forebody only in the presence of the wing and the forebody in isolation. The CHARM configuration and dimensions are shown in Figure 1

The chined forebody follows a tangent ogive planform with a fineness ratio of 3.00. The constant forebody cross section is defined using the super ellipse function, which results in a highly blended chined forebody which is asymmetric about its horizontal plane. This allows two model configurations to be tested by inverting the model in the cross flow. A third configuration is possible by changing the blowing direction, see Figure 2.

The forebody has a blowing slot in each chine edge which begins 0.10c downstream of the model apex and extends for 0.20c along each chine edge (where c is the forebody width, 100mm). Forebody configurations 1 and 2 utilise a slot which issues in the horizontal plane and forebody configuration 3 issues at 30 degress to the horizontal. The nominal width of the straight blowing slot is 0.0022c and the angled blowing slot is 0.0028c.

The two blowing slots are fed by independent plenum chambers. Each plenum chamber is connected via flexible tubing to a flowmeter, regulator and pressure source. This allows slot blowing momentum coefficients to be calculated for each blowing case.

Further details on the forebody and slot geometry, along with the calculation of blowing momentum coefficients and optimisation of the slot size are given by Williams [1].

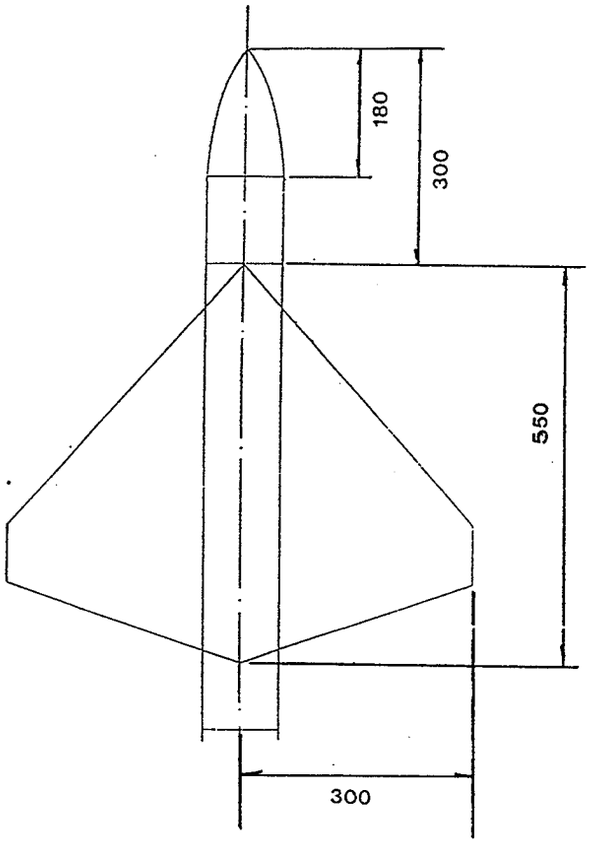

Figure 1. CHARM model configuration

To investigate the variation of blowing effectiveness with incidence a blowing rate was set and the model moved through an incidence sweep from 0 to 55 degrees with force data recorded at 5 degree intervals. This was done for blowing momentum coefficients (Cμ) between approximately 0.002 and 0.024.

To investigate the detailed effects of blowing momentum coefficient on the force data the model was set at a fixed incidence while the blowing rate was increased through nominally 5L/min steps. Force data was recorded through the entire blowing range for each blowing slot and also with wind-off so that the thrust effect could be measured.

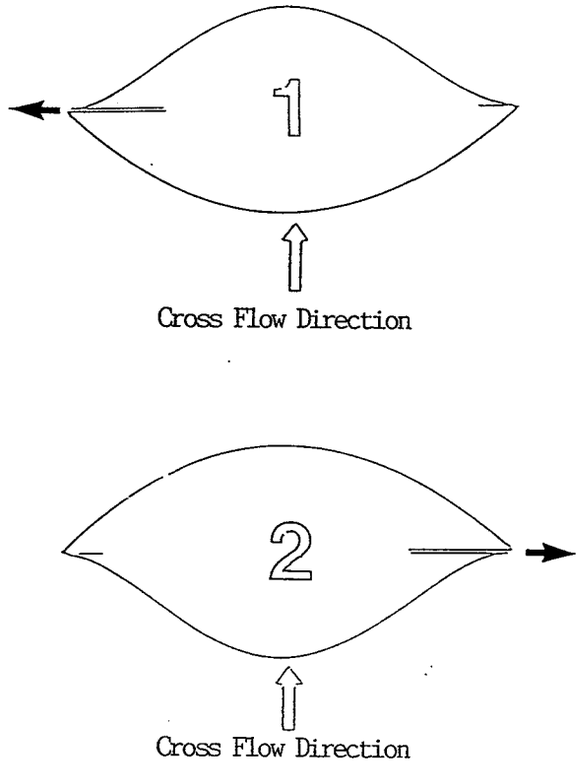

Experimental Procedure

The model is mounted on a sting which is clamped to a vertical support stem attached to the wind tunnel floor turn table through a mounting foot. The model is orientated with the wing in the vertical plane and with the balance reference point above the turn table centre. The vertical support stem for the sting has a simple elbow joint which can induce side slip angles but all the measurements reported here are at zero yaw.

The experimental procedure used took one of two basic forms:

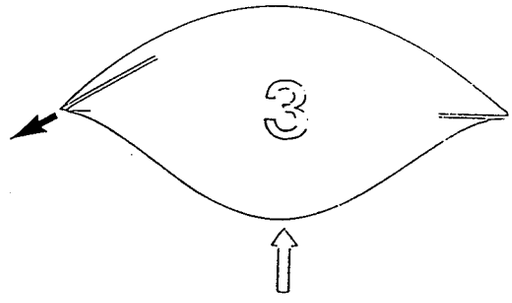

Figure 2. Forebody configurations 1 - 3

Results

This paper will concentrate on the results obtained for the complete forebody/wing model combination and make reference to the forebody in isolation data given in Garry [4].

All force and moment data is referenced to the gross wing area ($0.19m^2$) and mac (0.316m). The sign convention adopted is shown in Figure 3 with both the balance moment centre and model pitch axis positioned at 25% of the wing mac.

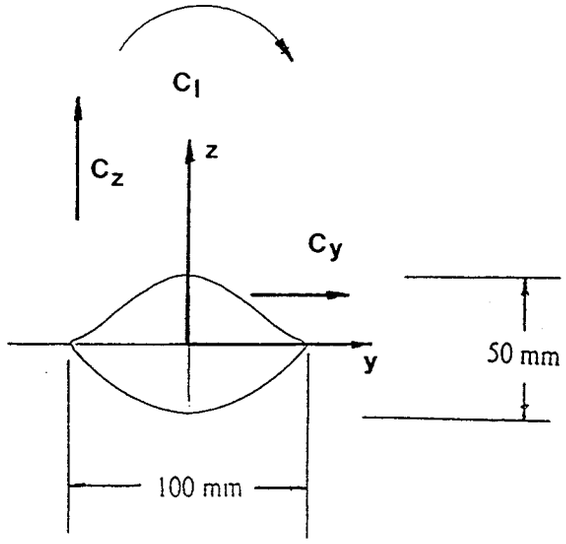

Figure 3. Force and moment sign convention, looking upwind.

Normal Force (C_z)

An example of the normal force generated by the forebody / wing combination, through the incidence range at various blowing momentum coefficients is shown in Figure 4. Blowing is seen to have a relatively small influence on the normal force for each of the three blowing configurations considered, the maximum increment occurring at approximately 40 degrees incidence. Blowing configuration 1 is seen to be marginally more effective at generating normal force increment than configurations 2 and 3.

Pitching Moment (C_m)

The influence of the forebody geometry is considerable if a comparison with the no blowing data is made between the three forebody configurations tested. Configurations 2 and 3 generate much greater nose up pitching moment at higher angle of attack. This is attributed to increased suction on the upper surface of the forebody for these two configurations, moving the model centre of pressure forward.

In general, blowing has little effect on the pitching moment generated by each configuration, although a trend is apparent in the results. At intermediate incidence 20 - 30 degrees, blowing reduces the nose up pitching moment, this then reverses between 30 - 45 degrees before more appreciable reductions in pitching moment occur above 45 degrees incidence, see Figure 5 for an example of this effect.

Figure 4. Effect of blowing on normal force coefficient through the incidence range at various blowing coefficients, forebody configuration 1.

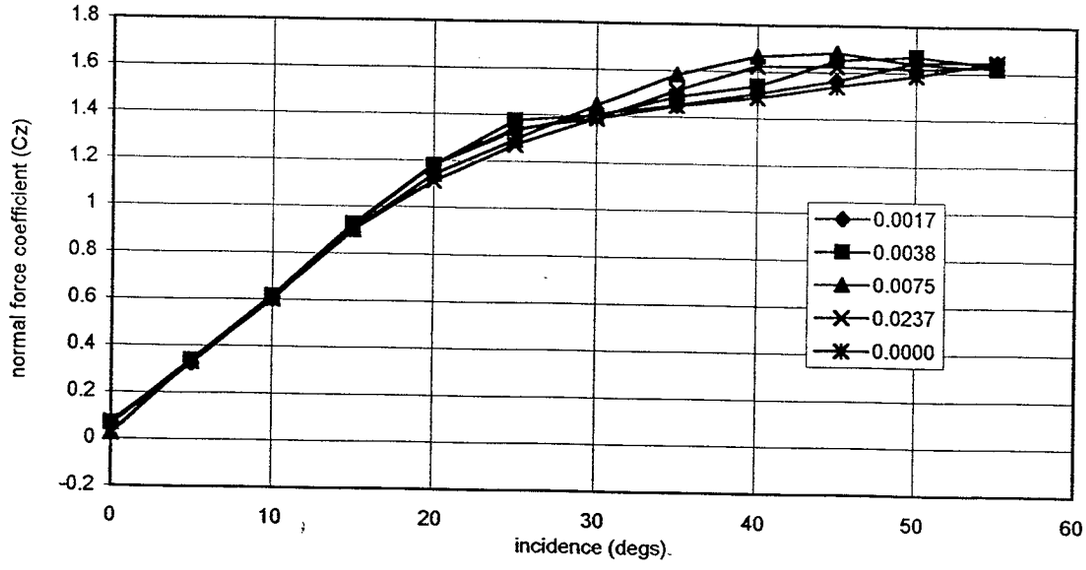

Figure 5. Increment in pitching moment coefficient, through the incidence range with thrust effect removed, at various blowing coefficients, forebody configuration 1.

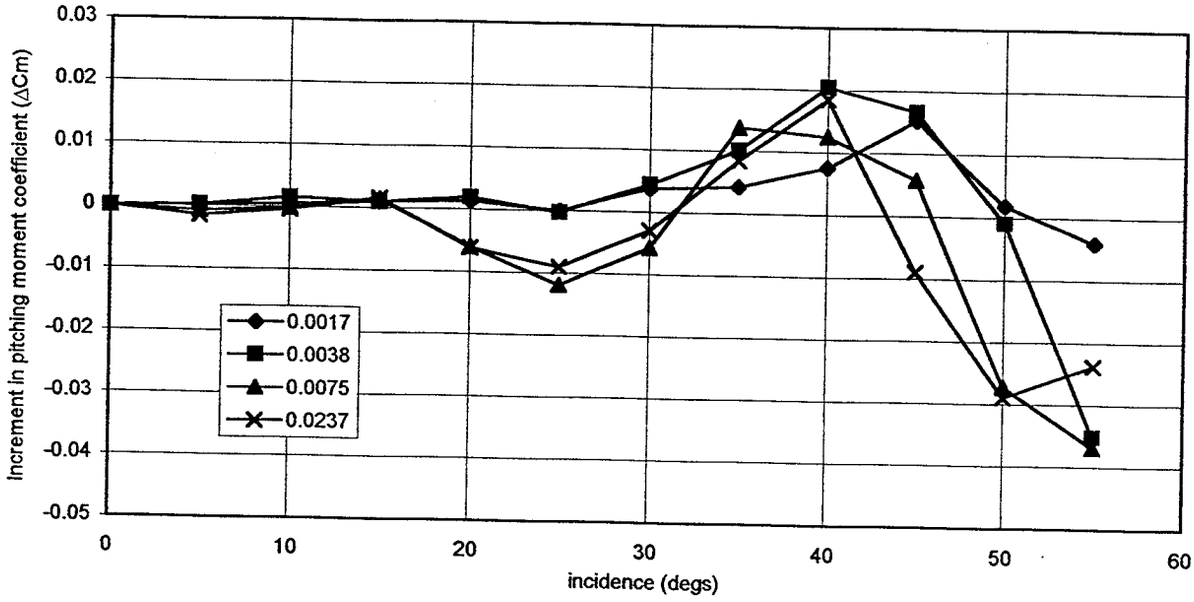

Side Force (C_y)

The model with no blowing should produce zero side force through the full incidence range but this was not the case. Small asymmetries are present in the vortex positions and burst points throughout the incidence envelope which are assumed to be due to either small asymmetries in model geometry near the forebody apex or possibly small side slip angles due to model alignment. This results in the non-zero side force coefficients observed when no blowing is present. The blowing jet thrust component of the side force was found to be constant throughout the incidence range for each blowing momentum.

Changes in side force coefficient due to blowing are significantly greater than that achieved through pure jet thrust, see Figure 6. This is assumed to be a result of

Figure 6. Increment in side force coefficient, with thrust effect removed, at various blowing coefficients, forebody configuration 1.

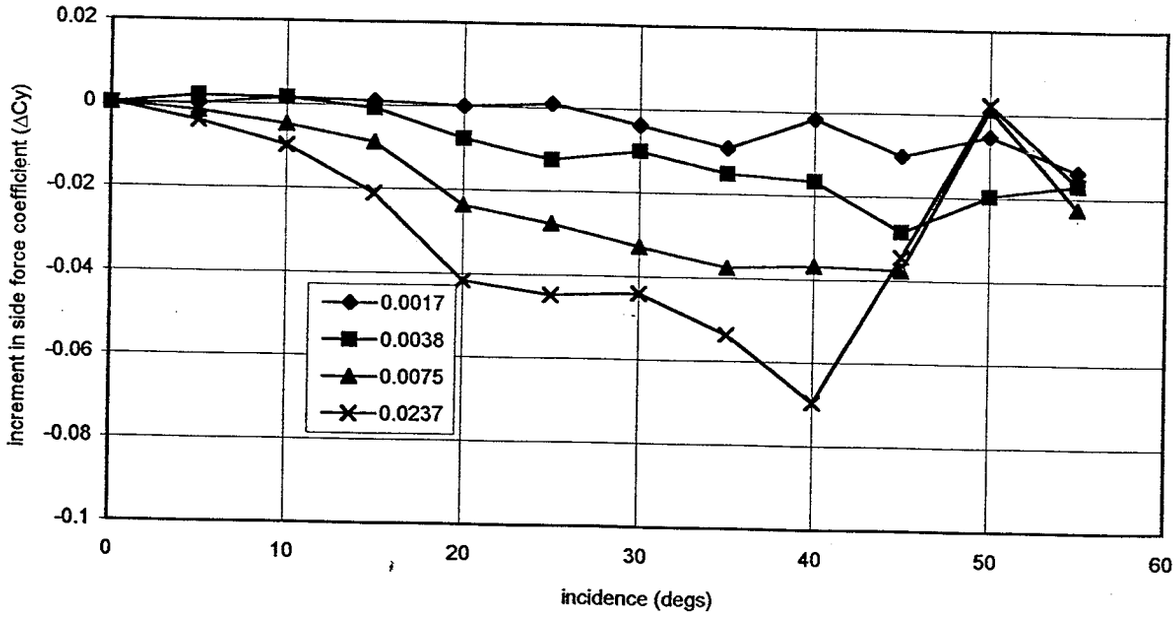

the displacement of the blowing side chine vortex which is seen to be moved up and away from the body. The consequent asymmetry in the vortex positions is then present down the full length of the model reducing the suction on the blowing side of both the forebody and afterbody, producing a resultant side force away from the blowing jet.

All three blowing configurations exhibit a point of inflection in the variation of side force with incidence at approximately 25 degrees which is believed to be due to the movement of the vortex burst position onto the afterbody / wing region - this reduces the area of the afterbody experiencing un-balanced suctions developed by the vortex asymmetry.

Analysis of the incremental side force data with blowing momentum coefficient at a given incidence shows side force increasing over the lower blowing momentum coefficient range and then becoming constant at the jet thrust component. Flow visualization results conducted by Williams [1] on the forebody in isolation have shown that blowing results in a movement of the blowing side vortex at the lower blowing momentum coefficients but at higher coefficients results in the blowing side vortex bursting. Further increments in blowing beyond this point produce no further flow asymmetry, the increments to' side force are purely jet thrust effects. Flow visualization has shown that a blowing jet vortex develops once the forebody vortex has burst. Initially this vortex is displaced away from the forebody and wing but as blowing increases further, it moves closer inboard.

Forebody configuration 3 - which uses down angled blowing - generally produces greater side force than the corresponding straight blowing configuration at the lower blowing momentum coefficients but is less effective at the higher blowing coefficients due to the earlier vortex bursting that is induced.

Yawing Moment (C_n)

An example of the yawing moment generated through the incidence range at various blowing momentum coefficients is shown in Figure 7 for forebody configuration 1. The results for each of the three forebody configurations considered are similar - each generates the highest yawing moment at 40 degrees incidence with the maximum blowing momentum coefficient. Flow visualisation shows that the forebody vortex bursts at this incidence suggesting that pressure changes on the forebody are primarily responsible for the yawing moment generated by blowing.

At incidences up to 35 degrees the blowing generates a gradual increase in yawing moment as the blowing side chine vortex is moved away from the model. This vortex eventually bursts, after which the yawing moment should remain constant except for further increments due to the jet thrust effect. There is little evidence of the blowing jet vortex at the higher blowing momentum coefficients.

At 45 degrees incidence, the same effect is apparent for forebody configurations 1 and 2 as for the side force

Figure 7. Increment in yawing moment coefficient, with thrust effect removed, at various blowing coefficients, forebody configuration 1.

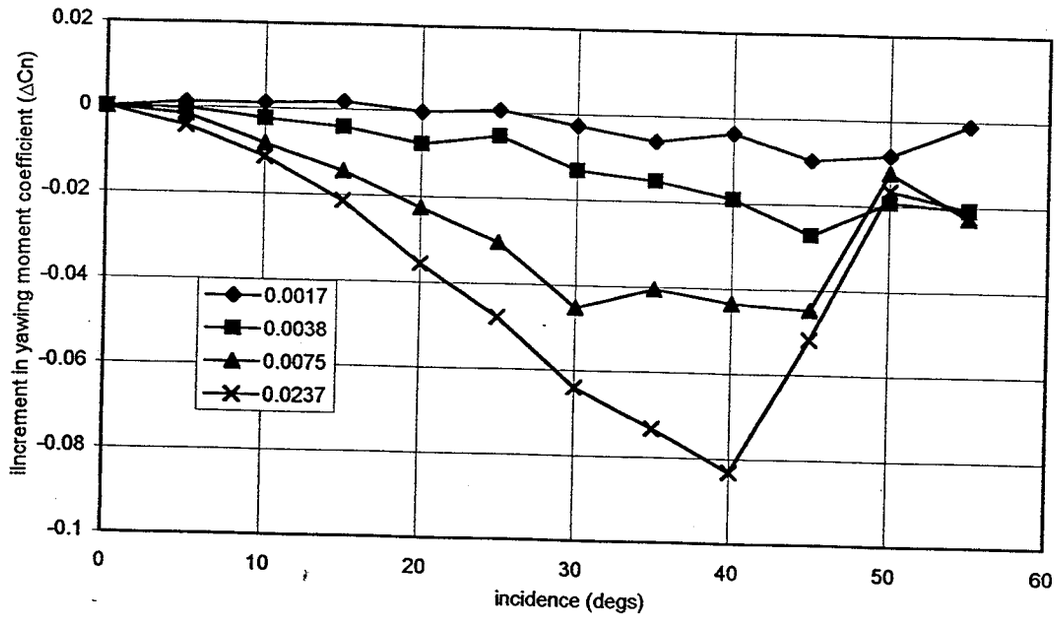

data. The yawing moment increases, reaches a peak before dropping to a more constant value. This is assumed to be the effect of vortex burst contaminating the non-blowing side vortex, reducing the suction on the forebody and hence the yawing moment. For configuration 1 however, a constant yawing moment is not achieved. As the blowing is increased further, at both 45 degrees and 55 degrees incidence, the yawing moment increases once again. This is assumed to be a consequence of the blowing jet vortex.

No firm conclusions can be made when comparing straight blowing through the two different model cross sections, although it is clear that down angled blowing once again causes vortex bursting before straight blowing for the same model cross section. The actual point at which bursting occurs does however appear to be a function of incidence, blowing direction, blowing momentum coefficient and model cross section.

Although there are small differences in the yawing moment generated by configurations 1 and 2 there is no clear advantage to either configuration as the trends are seen to vary through the incidence range.

Comparisons of down angled and straight blowing through the same model configuration show the same pattern of results as for side force data. At the lower blowing momentum coefficients the down angled blowing is more effective but as blowing momentum coefficient increases the straight blowing becomes superior. This is the case through most of the incidence range.

Rolling Moment without blowing

The no blowing response to incidence for each forebody configuration shows quite large rolling moments developing at 25 degrees (particularly for configuration 1), with a reversal above approximately 35 degrees. Flow visualisation shows asymmetry in the vortex burst location over the wing through the incidence range. For configuration 1, below 15 degrees incidence, there is no rolling moment induced on the model as the vortex burst of both the wing and chine vortices are down stream of the wing trailing edge. Between 15 and 20 degrees incidence the vortex burst points move onto the wing, and a rolling moment is induced as a result of asymmetry in the burst positions. At 25 degrees incidence the maximum rolling moment is developed as the chine and wing vortices interact. An asymmetry is present in both the wing vortex burst point and the chine vortex burst point which results in maximum rolling moment. Further increments in incidence see the burst points move further forward until at approximately 35-40 degrees incidence the whole wing vortex system has collapsed.

The magnitude of the no-blowing rolling moment for configurations 2 and 3 is much lower that for configuration 1. This suggests differences in the asymmetry in the wing vortex burst points for each configuration which may be due to the relative locations of the blowing slots but further work is needed to confirm this.

Rolling moment with blowing

Blowing generates considerable increments to the rolling moment encountered by the body, an example of which is given in Figure 8 for blowing configuration 1.

The basic flow mechanism is seen to be the same for all forebody configurations. When blowing takes place the blowing side chine vortex moves up and away from the body. This movement of the chine vortex occurs down the full length of the body. The movement of the blowing side chine vortex away from the blowing side wing vortex enhances the wing vortex, while the blowing moves the burst point of the non-blowing side chine and wing vortices further forward. This new vortex arrangement over the wing generates the rolling moment. If the blowing continues to increase the blowing side chine vortex will eventually burst. This does not effect the blowing side wing vortex, but does cause further forward movement of the burst point of the non-blowing side chine and wing vortices. Once the blowing side chine vortex has burst and if the blowing momentum coefficient is increased further a blowing jet vortex is generated which circulates in the opposite direction to the original chine vortex. This enhances the blowing side wing vortex even further.

The increments in rolling moment at 25 degrees incidence for configuration 1 are much lower than those seen on configuration 2 at the same incidence and with the same blowing momentum coefficient. This is assumed to be due to the asymmetry already present in the flow for configuration 1 but it is not possible to confirm this from the data available.

Configurations 2 and 3 show maximum rolling moment due to the blowing at 25 degrees, dropping off rapidly as the vortex burst moves further forward on the wing until between 35 and 40 degrees incidence the burst has moved to the wing apex. Further increments in incidence appear to reverse the effect of blowing.

The results for configuration 1 show a similar pattern but the magnitude of rolling moment changes at 25 degrees incidence due to blowing are much less than for configurations 2 and 3. This is thought to be either the result of the existing asymmetry in the flow at this incidence or the effect of the different forebody geometry. The increment in rolling moment beyond 35 degrees incidence is of a similar magnitude to that

Figure 8. Increment in rolling moment coefficient, with thrust effect removed, at various blowing coefficients, forebody configuration 1.

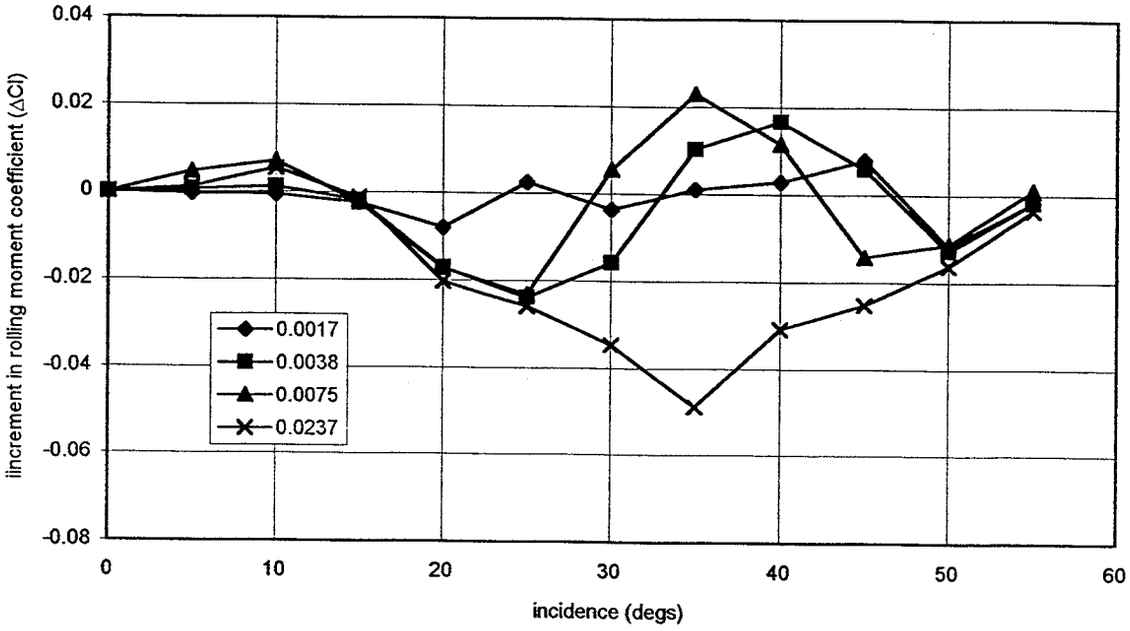

seen for configurations 2 and 3. This similarity may exist because of the fully burst nature of the wing flow field in this incidence range.

The results through the incidence range for the highest blowing momentum coefficient follow a slightly different pattern for all 3 configurations. This is thought to be due to the presence of the blowing jet vortex which appears once the chine vortex has burst.

At low incidence, below 15 degrees, all forebody configurations generate a rolling moment towards the blowing side. The vortex burst points are down stream of the wing trailing edge, hence the movement of the chine vortex with blowing has no effect on the burst points over the wing. The upward movement of the chine vortex on the blowing side reduces suction on the blowing side wing and hence generates a rolling moment in that direction.

Errors and repeatability

An analysis of possible errors generated by the 5 component strain gauge balance and the momentum coefficient calculations is given, for the forebody in isolation, by Williams [1]. The repeatability is a function of the unsteadiness of the flow structure through the incidence range. A simple repeatability test was conducted by taking 10 consecutive readings at each incidence with no blowing present and then at an intermediate blowing momentum coefficient. The spread of the force and moment data over these 10 readings gives an indication of the repeatability.

The spread of normal force and pitching moment data was found to increase through the incidence range, until maximum values of +/- 1% and +/- 2% respectively are reached at 55 degrees incidence. The presence of blowing had little effect on this spread.

The sideforce, rolling moment and yawing moment data show a similar trend but the spread of data is greater. The repeatability in side force shows a maximum spread of +/- 10% based on the highest sideforce coefficient. This is the result of the high degree of unsteadiness about the model at high angle of attack.

Conclusions

A series of low speed wind tunnel tests have been conducted on a generic combat aircraft research model to investigate pneumatic methods of yaw control at high alpha. Results have shown that blowing through slots in the chine edge near the forebody apex can produce significant yawing moments. Modification of the shear layer trajectory occurs when blowing is introduced which moves the blowing side chine vortex away from the body. The resultant vortex asymmetry generates both yawing moment and side force on the model with little coupling in normal force and pitching moment. However, significant roll coupling was measured as a result of enhancement of the blowing side wing vortex.

The yawing moment generated by blowing increases through the incidence range until a maximum is reached at approximately 40 degrees, above which blowing effectiveness reduces. Yawing moment also increases with blowing momentum coefficient at a given incidence. However, blowing beyond a certain coefficient only results in further yawing moment increments due to the jet thrust effect as a result of the bursting of the blowing side vortex.

The side force shows a similar pattern to the yawing moment results but exhibits relatively larger changes due to the contribution of the afterbody.

In contrast the rolling moment shows greatest coupling at 25 degrees incidence when the blowing side chine vortex moves off the body.

Investigations into the effect of blowing direction showed that downward angled blowing generates greater yawing moment increments than straight blowing at blowing momentum coefficients less than 0.075. Above this value the straight blowing is more effective.

Force component data indicates that the forebody generates the majority of the yawing moment. Testing the forebody in isolation will produce similar trends in yawing moment results but at a reduced magnitude. The rolling moment data showed that the forebody's contribution to the overall rolling moment was negligible compared to the wing roll component.

References

1. Williams, S.P., *An experimental investigation into yaw control at high alpha on a generic chined forebody using slot blowing* , Cranfield University, College of Aeronautics, MSc Thesis (1995).

2. Arena, A.S., Nelson, R.C., Schiff, L.B., *Lateral control at high angles of attack using pneumatic blowing through a chined forebody*, AIAA Paper 93-3624-CP.

3. Mendenhall, M.R., Lesieutre, D.J., *Prediction of subsonic vortex-shedding from forebodies with chines*, NASA CR-4323, September 1990.

4. Garry, K.P., Williams, S.P. Lateral control by tangential blowing through a chined forebody. Aero. Jn. Vol (100) 1996